NJC

PAPER

View Article Online
View Journal | View Issue





Cite this: *New J. Chem.*, 2018, **42**, 15346

# New model of metalloantibiotic: synthesis, structure and biological activity of a zinc(II) mononuclear complex carrying two enrofloxacin and sulfadiazine antibiotics†

Amina Boughougal,[ab] Fatma Zohra Cherchali,[ac] Amel Messai,[b] Nina Attik,[a] Dominique Decoret,[d] Maggy Hologne,[e] Corinne Sanglar,[e] Guillaume Pilet,[a] Jean Bernard Tommasino *[a] and Dominique Luneau [a]

Received 12th April 2018,
Accepted 6th August 2018

DOI: 10.1039/c8nj01774c

rsc.li/njc

A new model of the Zn-based complex, $[Zn(LH)(Erx)(ErxH)]ClO_4$ (sulfadiazine: LH and enrofloxacin ErxH), has been synthesised with two different, but complementary antibiotics (sulfonamide and quinolon) following an easy procedure. To evaluate the synergetic effect of this multicomponent molecule, the mononuclear complexes $[Zn(L)_2(H_2O)(NH_3)]$ and $[Zn(Erx)_3]^-$ which each include only one of the two antibiotics (sulfadiazine: LH or enrofloxacin ErxH) were synthesized. All three compounds were characterized, including crystal structure determination by single-crystal X-ray diffraction. For all of the complexes, enrofloxacin is coordinated to Zn(II) by pyridinone and one oxygen atom of the carboxylate group in a monodente mode. The antibacterial activity, determined by the minimum inhibitory concentration on specific bacteria, has been studied on free ligands, on the corresponding mononuclear complexes and on our model.

## Introduction

There is a significant amount of interest in elaborating new therapeutic models for transition metals described in the literature.[1] In the antimicrobial domain, the metalloantibiotic route that associates, all in one molecule, metal ions and organic antibiotics is recognized as being worthwhile. Owing to their multicomponent structure, these molecules can interact with several targets in the bacteria leading to a specific and unique bioactivity mechanism.[2] With this in mind, the coordination of metal ions by antibiotics as ligands remains to be a major challenge that needs to be addressed in order to improve the antimicrobial effect.[3] Large molecular designs of metal complexes have been reported in the literature, in particular with silver, copper or zinc ions.[4] Most of them are mononuclear and neutral, but a few dinuclear molecules have also been reported.[5]

For the past few years, exploring the synthesis of such metalloantibiotics and the synergetic effect due to this association has been an active field of research for us.[6] Concerning the antibiotics playing the role of the ligand, our interest has been focused on the sulfonamides and quinolones (Scheme 1) which are an important class of antimicrobial agents and are used in both human and veterinary medicine.[7]

Moreover, sulfonamides, in various substituted forms, have donor atoms that make them excellent and versatile ligands, providing different coordination modes with metallic ions.[8] As well as this, the keto-carboxylic acid groups present in quinolone and fluoroquinolone types of molecule give diversity to molecular architectures that have a bidentate binding mode, but also those with a tridentate coordination mode due to the presence of a piperazine group.[9]

In the fight against bacterial resistance and to prevent the development of "nosocomial" diseases, novel strategies have

[a] *Université de Lyon, Laboratoire des Multimatériaux et Interfaces (LMI) UMR 5615 CNRS – Université Claude Bernard Lyon 1, avenue du 11 novembre 1918, 69622 Villeurbanne Cedex, France. E-mail: jb.tommasino@univ-lyon1.fr*
[b] *Laboratoire d'Ingénierie et Sciences des Matériaux Avancés (ISMA), Institut des Sciences et Technologie, Abbès Laghrour University, Khenchela 40000, Algeria*
[c] *Laboratoire d'Etudes Physico-Chimiques des Matériaux, Application à l'Environnement (LEPCMAE), USTHB, Faculté de Chimie, Bab Ezzouar, Algeria*
[d] *UFR Odontologie, Université Lyon, Université Lyon1, Lyon, France*
[e] *Univ. Lyon, CNRS, UCB Lyon 1, Institut des Sciences Analytiques, UMR 5280, 5 rue de la Doua, 69100 Villeurbanne, France*

† Electronic supplementary information (ESI) available. CCDC 1836021 and 1836022. For ESI and crystallographic data in CIF or other electronic format see DOI: 10.1039/c8nj01774c

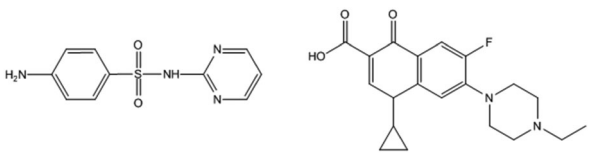

Scheme 1 (a) Sulfadiazine (LH) and (b) Enrofloxacin (ErxH) are examples of antibiotics of the sulfonamide and quinolone types respectively.

 

been proposed. For example, ''bi-therapy'' treatments, based on a cocktail formulation of two antibiotics with a synergic effect, are currently used in hospitals.[10] In a continuation of our previous work,[6] we hypothesized that coupling, within one metal complex, both a sulfonamide and a quinolone antibiotic that have complementary biological activities could be an interesting alternative. Furthermore, our hypothesis was that such a complex may have an even better antibacterial activity than a simple cocktail of the two. Bearing this idea in mind, we were expecting an exhausted synergetic effect due to the all-in-one association of an antiseptic metal ion with the two antibiotics. From the possible metal ions that could be used, we choose zinc as it is a recognized antiseptic[11] and the second most abundant d-block natural metal ion in humans.[12] Zinc has been the topic of several studies, demonstrating its key role in metalloenzymes and/or metallopharmaceutics.[13] Moreover, several zinc antibiotic complexes have been reported in the literature with either an O-donor or N-donor co-ligand.[4] This includes, for example, the monomers of $[[Zn(Aza\text{-}f)(Erx)]NO_3]$,[14] $[Zn(erx)_2(Phen)_2]$,[15] $[Zn(erx)_2(py)_2]$[16] (erx: enrofloxacin, Aza-f: azabis(oxazoline, py: pyridine, Phen: 1,10 phenanthroline) and $[Zn(flmq)_2(bipy)]$[4] (flmq: flumequine, bipy: bypiridine) or the dimer $[Zn_2(levofH)_2(odpa)]$,[17] (odpa = 4,4_-oxydiphthalate, levofH = levofloxacin)). In these complexes, the only role of the co-ligand is to stabilize the structure around the metal ion.

In this paper we describe a quick and easy synthesis route to isolate a zinc/erx/L (**3**) model (L: sulfadiazine). To the best of our knowledge, this is the first synthesized molecule combining two different antibiotic ligands within one coordination complex. For biological activity comparison purposes we also synthesized $[Zn(L)_2(H_2O)(NH_3)]$ (**1**) and $[Zn(Erx)_3]^-$ (**2**) mononuclear metalloantibiotic complexes, integrating only one type of antibiotic: sulfadiazine (L) or enrofloxacin (Erx). All three complexes **1–3** were fully characterized by infrared (IR) and NMR spectroscopies and structural determination was carried out using X-ray diffraction on single crystals (**1** and **3**). This is an important aspect as knowledge of the crystal structure of a drug, without any ambiguity, and the different metal cation coordination modes are key points that need to be determined to understand the interactions with bacteria. The antimicrobial activities of the three complexes (**1–3**) have been assessed against three bacteria strains *Escherichia coli*, *Staphylococcus aureus* and *E. faecalis*. Finally, a comparative study was carried out on the parent antibiotic alone.

# Results and discussion

### Synthesis

Enrofloxacin has an ionisable carboxylic acid group with a $pK_{a_1}$ value of around 5 and a basic piperazinyl group with a $pK_{a_2}$ value between 8–9.[18] Therefore, depending on the pH of the solution, enrofloxacin can be either an anion (deprotonated), a zwitterion or a cation (protonated). In a mixture of ammonia and ethanol, and by addition of a concentrated $NH_3$ solution, the deprotonation of both groups leads to an anionic species with a charge delocalization to a neighboring keto moiety, allowing the stabilization of the species by a hydrogen bond. The metallic ion precipitates first with the formation of $Zn(OH)_2$, which is dissolved by an excess of ammonia to form $[Zn(NH_3)_4]^{2+}$. Slow evaporation of the ammonia gas provides favorable conditions for obtaining coordination of the metal ions.[6,19] This bidentate mode of coordination through the pyridone oxygen and a carboxylate oxygen atom is already known with others quinolones.[9,16,20] With a similar synthesis procedure, the coordination modes of the platinium group metal (PGM) observed with levofloxacin (methyl group substituted to the piperazine nitrogen) seems to demonstrate that the metallic ions can also be linked through the nitrogen atom of 4-methylpiperazin-1-yl moiety,[21] in contrast to our observations.

Using the same conditions, a large family of complexes can be obtained with sulfonamide ligands, highlighting the advantages of this method.[6]

The mixture of these three species, enrofloxacin, sulfadiazine and $Zn(ClO_4)_2$, leads to the first mixed all-in-one complex combining two enrofloxacins and one sulfadiazine ligand with the cationic zinc. After slow evaporation of the solvent over five days, colourless single-crystals can be isolated and characterized using X-ray diffraction. In order to establish a comparative study, we also synthesised the corresponding complexes with only one type of antibiotic ligand. Therefore, following the same experimental procedure, two new complexes; Zn/enrofloxacin and Zn/sulfadiazine, have been elaborated and characterized using single-crystal X-ray diffraction.

### Crystal structure

Using the synthesis method described above, three original complexes based on two antibiotic ligands, enrofloxacin ErxH and sulfadiazine LH, were obtained. In the case of complex **2**, a complicated statistical disorder of the counter-cation within the unit-cell prevented us from completely refining the structure. The results presented below for **2** are only those obtained for the inorganic anionic metallic heart and are presented here as a model. In the case of complex **3**, a twin law has been applied and the proportion of the two components has been refined to 0.687 and 0.313. The chemical formulae for the complexes are as follows: 1: $[Zn(L)_2(H_2O)(NH_3)]$; 2: $[Zn(Erx)_3]^-$ and 3: $[Zn(LH)(Erx)(ErxH)]ClO_4$. For all compounds, X-ray powder diffraction was performed on several milligrams of each sample and compared to the theoretical powder diagrams generated from the crystal structures to confirm the homogeneity of the sample (see Fig. SI5–SI7, ESI†).

**Crystal structure description of 1.** The complex crystalizes in the non-centrosymetrical $Pna2_1$ orthorhombic space group with a Flack parameter equal to 0.11(2). The Zn(II) metal center is located in a distorted $ML_5$ $\{O_1N_4\}$ square-base pyramidal environment and coordinated to two $L^-$ deprotonated ligands, one $H_2O$ molecule and one $NH_3$ solvent molecule (Fig. 1a). Zn–N bond lengths range from 2.049(5) Å to 2.413(5) Å and the Zn–O bond length is equal to 2.034(6) Å. For both ligands, the $-NH_2$ terminal groups, responsible for the biological activity, are not involved in any direct coordination to any metal center.

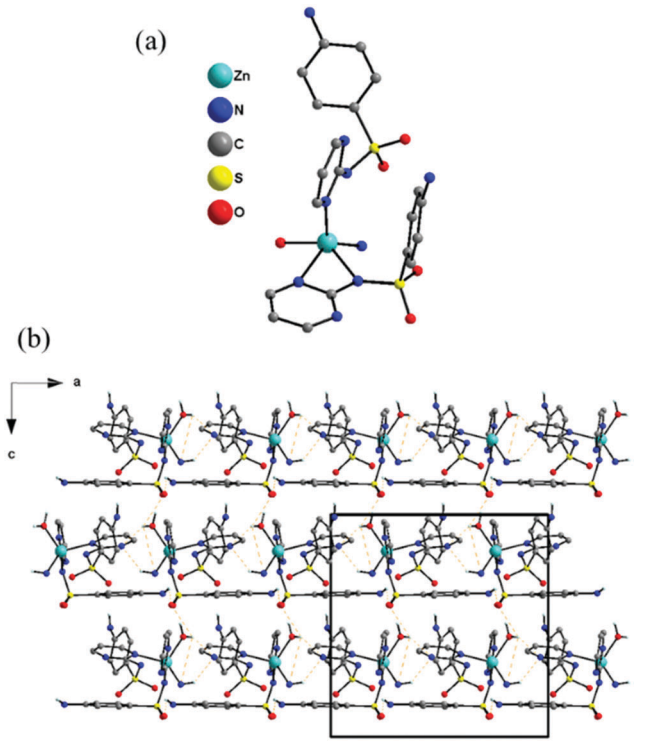


Fig. 1 (a) Complex **1**. For clarity, the hydrogen atoms have been removed; (b) structure packing projection perpendicular to the *b*-axis of the unit-cell. Hydrogen bonds are represented in orange dashed lines. Only hydrogen atoms involved in hydrogen bonds have been represented.

The structural cohesion is ensured by the presence of several hydrogen bonds (N/O–H···O/N) which leads to a dense 3D network (Fig. 1b).

**Crystal structure model of anionic inorganic moiety 2.** The complex crystallizes in the trigonal centrosymetrical $R\bar{3}$ space group. The metal center, $Zn^{2+}$, is coordinated to three deprotonated Erx ligands. The Erx ligands are coordinated to the cation through the β-dicetone function and not the acid one.

This mode of coordination was confirmed by IR spectroscopy (see Table 1). The band at 1700 $cm^{-1}$ that is characteristic of the valence vibration of the carboxylic stretch has disappeared and has been replaced by two new strong bands at 1568 and 1388 $cm^{-1}$ assigned to O–C–O vibrations.

The $Zn^{2+}$ metal center is localized in a slightly distorted $ML_6$ $\{O_6\}$ environment in which the Zn–O bond lengths range from 2.044(2) Å to 2.121(2) Å (Fig. 2).

**Crystal structure description of 3.** The complex crystallizes in the centrosymetrical triclinc $P\bar{1}$ space group. The metal center, $Zn^{2+}$, is coordinated to one neutral LH ligand and two Erx ligands, one protonated (neutral) and one deprotonated (with a statistical 50 : 50 distribution of the hydrogen atom on both the acid groups of the two Erx ligands, see further details in the discussion of the NMR spectra). Then, a cationic $[Zn(LH)(Erx)(ErxH)]^+$ metallic heart (Fig. 3a) is formed and the charge balance is ensured by the presence of one $ClO_4^-$ counter-anion. The metallic center, $Zn^{2+}$, is located in an almost perfect $ML_5$ $\{O_4N\}$ square-base pyramidal geometry. The four oxygen atoms belong to the acid groups of the two Erx ligands and the nitrogen atom comes from the L ligand. The Zn–O/N bond lengths are close to each other and range from 1.983(4) Å to 2.124(4) Å. It should be noted that the terminal $–NH_2$ of the ligand L, responsible for the biological activity, is not involved in any coordination with any metal center.

Table 1 Infrared spectroscopy of complexes **1**, **2** and **3**

| $cm^{-1}$ | $\nu(C{=}O)_{carb}$ | $\nu(C{=}O)_{asym}$ | $\nu(C{=}O)_{sym}$ | $\nu(C{=}O)_p$ | $\Delta$ |
|---|---|---|---|---|---|
| **2** | | 1568 | 1388 | 1620 | 180 |
| **3** | | 1580 | 1388 | 1630 | 192 |
| Erx | 1734 | | | 1615 | |
| | $\nu_{as}(NH_2)$ | $\nu(SO_2)$ | $\nu(NH_2–Ph–)$ | $\nu(C–S)$ | |
| **1** | 3350–3420 | 1260 | 1578 | 680 | |

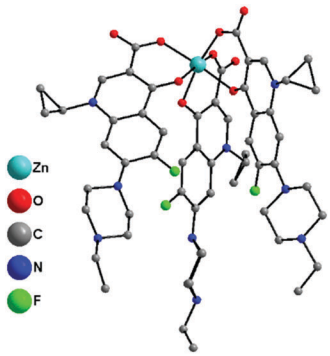


Fig. 2 Anionic metallic inorganic moiety of complex **2**. For clarity, hydrogen atoms have been removed.

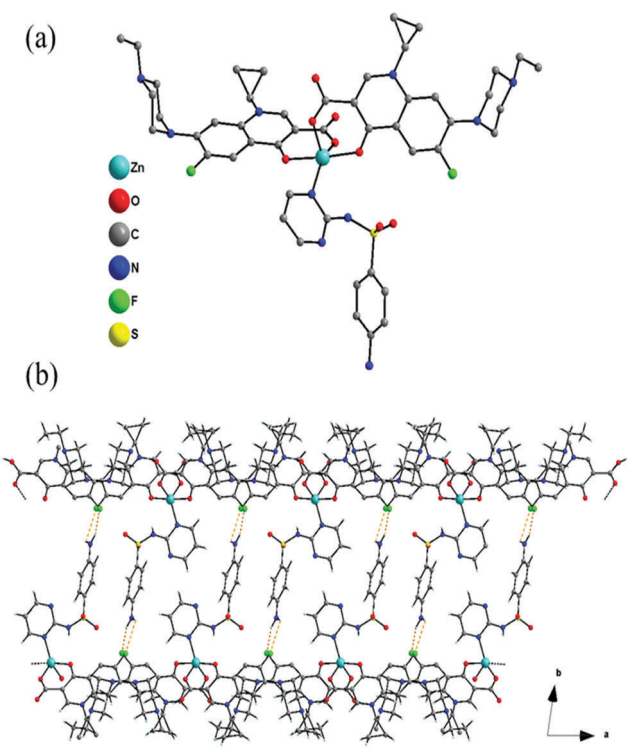


Fig. 3 (a) Cationic complex **3**. For clarity, hydrogen atoms have been removed. (b) Illustration of the F···H interactions (orange dashed lines) generating chains of complexes running along the *a*-axis of the unit-cell.

 

The presence of F···H interactions (between the L and Erx ligands, respectively) generate the formation of pseudo-chains of complexes running along the *a*-axis of the unit-cell (Fig. 3b). The structural cohesion between these chains is ensured by hydrogen bonds involving the $ClO_4^-$ counter-anions, the NH groups of the L ligands and the hydrogen atoms of the acid groups belonging to the Erx ligands to form a dense 3D network.

### NMR spectroscopy

1D $^1$H NMR spectra were recorded for the different samples: free sulfadiazine, free enrofloxacin, and complexes **2** and **3** (Fig. 4). In the spectra for **2**, we do not observe any signal for the acid proton compared to the free form case ($\delta_{COOH}$ = 15.16 ppm). The complex is therefore deprotonated in solution. In contrast, in the case of complex **3**, a signal at 15.16 ppm is present. The complex has two Erx ligands, but the integration of this signal is only 1. This means that there is only one protonated Erx ligand in this complex. These observations are in agreement with the single-crystal X-ray diffraction refinement results. There are no chemical shift perturbations for free and complexed sulfadiazine ligands (Fig. 4a and d). Some perturbations in the chemical shifts of enrofloxacin are observed owing to the complex formation and conformational rearrangement. In particular, the $^1$H at 8.65 ppm (H15) is a singlet in the free form and splits into two broad peaks in complex **2** and into two sharp peaks in complex **3** (Fig. 4h–j). In the latter case, we could measure the two integrations of each peak to 1. Moreover, in the 1D $^{19}$F spectrum, two distinct signals are observed (Fig. 4m) and the integration is determined to be 1 for each of them. Those two results indicate that the two Erx ligand of complex **3** are different: one of the two ligands is protonated. For complex **2**, it is impossible to deconvolute the signal of H15, but the full integration is 3. The $^{19}$F signals exhibit the same broadening (Fig. 4l). The integration ratio is 2 : 1 between the two peaks at −123.7 and −124.7 ppm, respectively. The broadening of the peaks is characteristic of an intermediate exchange rate between the two conformers of the complex. The population of the two positions is given by the integration ratio 2 : 1. During the NMR time scale, one of the Erx ligands is probably rotated compared to the two other ligands.

The same features are also visible in the case of the H18 of Erx: a doublet in the free form, then a broadening of the signal occurs in complex **2** and we see two distinct doublets for complex **3**. These results corroborate the fact that there are two different orientations for the Erx ligand with a ratio of 2 : 1 for complex **2** and a ratio 1 : 1 for complex **3**.

### Infrared spectroscopy

The IR spectroscopy study focused on the quinolone ligand responses. Indeed, the coordination mode of the quinolone ligand in the complex can be clarified by the study of the characteristic bands. Typical bands at 1700 cm$^{-1}$ and 1630 cm$^{-1}$ characterize the spectrum of the enrofloxacin ligand, the valence vibration $\nu$(CO) of the carboxylic stretch and the $\nu$(CO) of the quinolone stretch (Table 1, also see Fig. S8 in the ESI†). Within the complexes, this valence vibration of the carboxylic stretch disappeared and was replaced by two new strong bands at

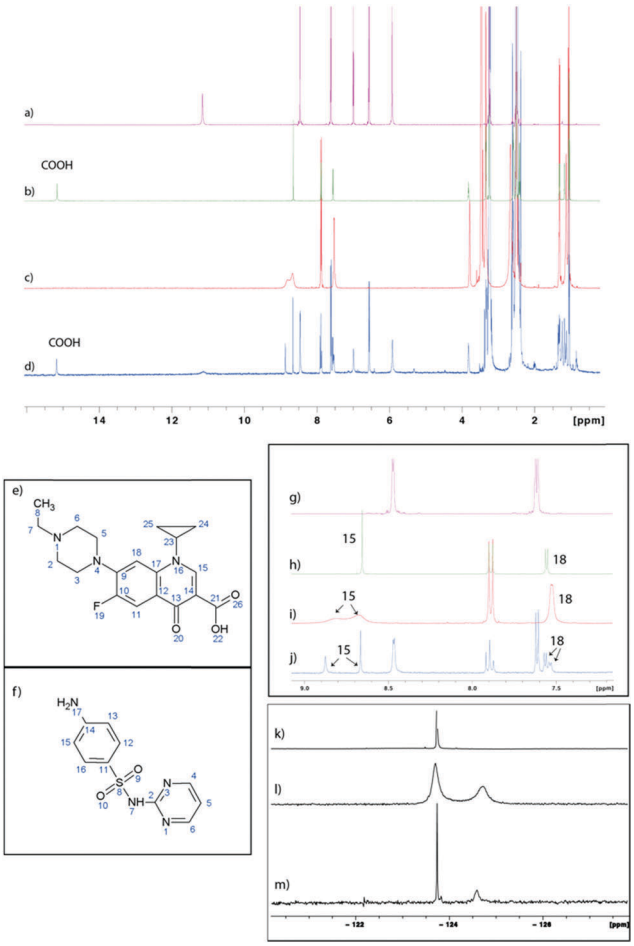


Fig. 4 Full 1D $^1$H NMR spectra of (a) free sulfadiazine; (b) free enrofloxacin; (c) complex **2**; and (d) complex **3**. (e) Structure of Erx with atoms numbering; (f) structure of sulfadiazine with atoms numbering. 1D $^1$H aromatic region spectrum of (g) free sulfadiazine; (h) free enrofloxacin; (i) complex **2**; and (j) complex **3**. Numbers of characteristic $^1$H from Erx are included in the Fig. 1D $^{19}$F NMR spectra of (k) free Erx; (l) complex **2**; and (m) complex **3**.

1568 and 1388 cm$^{-1}$ which were assigned to the carboxylic $\nu$(CO) vibrations in the complex:[1,20] the asymmetric $\nu(CO)_{carb}$ and symmetric $\nu(CO)_{carb}$. Generally, the difference between these two bands can define the coordination mode of the carboxylate function, which is monodentate or bidendate.[22] In this instance, this difference, varying from 180 cm$^{-1}$ to 220 cm$^{-1}$, seems to confirm a monodentate coordination mode of the carboxylate group.[23] In our case, the $\nu$(CO) stretch moves between 10–20 cm$^{-1}$. We propose that the metal ion is coordinated with one of oxygen atoms of the carboxylate group and with the oxygen atom of the pyridinone moiety. The IR spectra measurement in DMSO solution shows a similar pattern and confirms the stability of the complex in solution.

### Minimum inhibitory concentration

The results obtained for the free ligands of enrofloxacin, sulfadiazine, complexes **1** and **2** and model **3** samples against *E. coli*, *S. aureus* and *E. faecalis* bacteria strains are detailed in Table 2. The data shows that all samples expressed a similar or

Table 2 Minimal inhibitory concentration (MIC), (mg $L^{-1}$) of the free ligands enrofloxacin, sulfadiazine, complexes **1** and **2** and published complexes compared to the model of **3**

| | *E. coli* | *S. aureus* | *E. faecalis* |
|---|---|---|---|
| Enrofloxacin | 0.5 | 8 | 8 |
| Sulfadiazine | 128 | 8 | >256 |
| **1** | 1 | 256 | 256 |
| **2** | 0.5 | 2 | 16 |
| **3** | <0.5[a] | <0.5[a] | <0.5[a] |
| [Zn(Erx)(Phen)Cl][16] | 10 | 2 | |
| $[Co(Erx)_2(H_2O)_2]$[23a] | 1 | 2 | |
| $[Ni(Erx)_2(H_2O)_2]$[23b] | 1 | 8 | |
| $[Zn(Erx)_2(H_2O)]$[23a] | 1 | 2 | |
| $[Cu(Erx)_2(H_2O)]$[23c] | 0.125 | 4 | |

[a] Here, the MIC is inferior to 0.5 mg $L^{-1}$, which is beyond the limits of our study.

a better activity *versus* the free antibiotic ligand. The minimum inhibitory concentration (MIC) results obtained with complexes **1** and **2** are in agreement with the complexes synthesized and studied in the literature.[16,20,22,23] From Table 2, the complexes seem to slightly improve the antibacterial activity with regards to the free bioligands. Concerning the sulfonamide, we have already demonstrated these same trends for copper and nickel complexes in previous work.[6] We have observed similar behavior with different zinc complexes with several sulfonamide ligands. Usually, in the case of quinolone, it is demonstrated that the complexes of sparfloxacin, enrofloxacin and *N*-propyl-norfloxacin are more active than oxolinic and pipemidic acid.[22] As can be seen in Table 2, the copper(II) complex $[Cu(Erx)_2(H2O)]$[23a] seems to be the most active against *E. coli*, with a MIC value of 0.125 mg $L^{-1}$. However, the other quinolone complexes have similar MIC values for the bacteria described here from 1 to 10 mg $L^{-1}$.

The elaborated model of **3** has a greater efficiency for all the bacteria tested in our work in the range of the studied concentration with a MIC value that is probably lower than 0.5 mg $L^{-1}$, the lowest limit value in our study. Moreover, the model seems to be more effective than the other molecules found in the literature (see Table 2). Although it seems difficult to give a clear explanation of the mechanism and role of the metal in penetrating the membrane, it appears that the synergetic effect of each entity in our model of **3** strongly increases its activity. The fact that **3** is a cationic entity should contribute to this efficiency: the interaction with the lipoidal bacterial membrane could be suitable to achieve enhanced penetration. This last consideration could be an important parameter which would add to the synergic effect of the two antibiotics in the molecule.

## Conclusions

In this work, a new concept for a metalloantibiotic synthesis associating two types of antibiotic as ligands, and exhibiting a synergetic effect and an antiseptic central cation has been developed and named as multi-active biomolecule assembly (complex **3**). This Zn(II)-based complex, which can be easily synthesized, shows MIC activities (*E. coli*, *S. aureus*, *E. faecalis*) which are between 2–20 times better than those presented in the literature, to the best of our knowledge. Although the antibiotics presented in this article are probably not an optimal association, our results highlight that this new concept could be promising and could open a new bright pathway towards a new family of bioactive molecules based on coordination chemistry.

## Experimental section

### General procedure for complexes synthesis

A solid and defined mixture of the $Zn(ClO_4)_2$ metal salt, sulfadiazine and/or enrofloxacin was dissolved in 5 mL of methanol Then, a concentrated ammonia solution (25%) was added dropwise until the apparition and the subsequent disappearance of a white precipitate. The resulting solution was stirred for 10 min. After 2–5 days of slow evaporation of the solvent at room temperature, single-crystals (white for both of the complexes) were obtained which were suitable for X-ray data characterizations. 1: Yield: 66%, Anal calc. C, 40, 10; H, 3, 87; N, 21, 05. Found: C, 40, 15; H, 3, 76; N, 20, 94; 2: Yield: 77%, Anal calc. C, 54, 36; H, 5, 76; N, 10, 01. Found: C, 54, 15; H, 6, 21; N, 10, 04; 3 Yield: 37%, Anal calc. C, 50, 89; H, 4, 72; N, 12, 36. Found: C, 50, 85; H, 4, 82; N, 12, 45.

### Instrumentation and characterization

FT-IR spectra were performed from 4000 to 200 $cm^{-1}$ with a Nicolet 380 FT-IR spectrometer coupled with the attenuated total reflectance (ATR) accessory. The powder X-ray diffraction (PXRD) was performed on a PANanlytical XpertPro MRD diffractometer.

### Single-crystal X-ray diffraction

Single-crystal X-ray studies of complexes **1–3** were carried out using a Gemini diffractometer and the related analysis software, respectively.[24] An absorption correction based on the crystal faces was applied to the data sets (analytical).[25] The structures were solved by direct methods using the SIR97 program[26] combined with Fourier difference syntheses and refined against $F$ using reflections with $[I/\sigma(I) > 3]$ by using the CRYSTALS program.[27] All atomic displacement parameters for non-hydrogen atoms were refined with anisotropic terms. The hydrogen atoms were theoretically located on the basis of the conformation of the supporting atom and refined by using the riding model. CCDC 1836021–1836022. X-ray crystallographic data and refinement details for complexes **1–3** are summarized in the ESI† Table SI 1. Important bond lengths, bond angles as well as intra- and inter-complexes distances are collated in Tables S2 and S3 (ESI†).

### Minimum inhibitory concentration

The antibacterial activity of the metalloantibiotic complex samples was assessed *in vitro* against three bacterial strains: *Escherichia coli* (CIP 54127), *Staphylococcus aureus* (CIP 4.83) and *E. faecalis* (CIP 103214) (Institut Pasteur, Paris, France). These strains were selected in order to represent Gram-negative

 

and Gram-positive bacteria responsible for nosocomial infections and hospital-acquired Illnesses. A standard method with a 96-well dilution technique was used for the determination of the MIC of the tested samples. Five samples were tested (free ligands enrofloxacin, sulfadiazine, complexes **1** and **2** and model **3**). Owing to the insolubility of the samples in water, they were dissolved in dimethylsulfoxide (DMSO) at 20%. For each species, a pre-cell culture of bacteria was grown in brain heart infusion medium (BHI) for 36 h at 37 °C. Three dilution series ranging from 0.5 to 256 mg $L^{-1}$ in BHI was performed for each sample with a final volume of 1 mL and a final DMSO concentration of $\leq$2%. The concentration of DMSO decreases with serial dilution. Moreover, a solution without any active complexes at a 2% DMSO concentration was tested and did not influence the bacterial growth. Then, 1 mL of the bacteria suspension prepared in BHI at the optical density of $OD_{600}$ = (0.5–0.6) measured using a spectrometer (Helios Epsilonspectrophotometer, Thermo Spectronic, Rochester, NY, USA) was added to each of the tested samples. As a negative control, the bacteria suspension without samples was incubated and treated in the same conditions. The bacterial growth corresponding to the samples turbidity was determined by measuring the absorbance of the samples at 600 nm using a microplate reader (Infinite® F200, Tecan group LTD. France) after 24 h incubation at 37 °C for both the control and tested samples. The results were expressed as concentration (mg $L^{-1}$). Three independent experiments were carried out for each sample.

### NMR spectroscopy

Each sample was prepared as follows: 6 mg of product (ligand and complex) were dissolved into 600 μL of DMSO-$d_6$. $^{19}$F NMR spectra were recorded on a Bruker Avance III HD 400 MHz operated at 376.45 MHz spectrometer equipped with a 5-mm PABBO BB/$^{19}$F–$^{1}$H/D probe with z-gradients. Acquisition sequences for 1D NMR $^{1}$H, $^{13}$C, DEPT 135 and 2D NMR experiments COSY, HSQC and HMBC were recorded on a Bruker Avance III HD 600 MHz spectrometer equipped with a 5 mm TXI H-C/N-D probe with *z*-gradients. The sample temperature was regulated at 40 °C. $^{19}$F experiments were recorded using 13.7 μs pulse (90°), a delay time of 4 s, an acquisition time of 1.7476 s and the number of scans was 120. Data were processed using 1 Hz line broadening. 1D et 2D homo- and heteronuclear experiments were recorded using an 8 μs pulse (90°, $^{1}$H), a spectral width of 9615.38 Hz for the proton and 13 μs pulse (90°, $^{13}$C), a spectral width 36057.69 Hz for the $^{13}$C. Chemical shifts of the different samples are given in the supplementary information.

## Conflicts of interest

There are no conflicts to declare.

## Acknowledgements

The authors acknowledge the French-Algerian Tassili PHC Programme N° 15MDU940 for the financial support and Dr Karen Moreau from the University of Lyon, for her kind advices about the antibacterial activity assessment.

## Notes and references

1 I. Turel, *Coord. Chem. Rev.*, 2002, **232**, 27–47; L. J. Ming, *Med. Res. Rev.*, 2003, **23**(6), 697–762.
2 J. W. Grate and G. C. Frye, in *Sensors Update*, ed. H. Baltes, W. Göpel and J. Hesse, Wiley-VCH, Weinheim, 1996, vol. 2, pp. 10–20; R. Saraiva, S. Lopes, M. Ferreira, F. Novais, E. Pereira, M. J. Feio and P. Gameiro, *J. Inorg. Biochem.*, 2010, **104**, 843–850.
3 S. M. Mandal, A. Roy, A. K. Ghosh, T. K. Hazra and O. L. Franco, *Front. Pharmacol.*, 2014, **5**, 1–12; G. Kerbauy, A. C. P. Vivan, G. C. Simões, A. S. Simionato, M. Pelisson, E. C. Vespero, S. F. Costa, C. G. T. J. Andrade, D. M. Barbieri, J. C. P. Mello, A. T. Morey, L. M. Yamauchi, S. F. Yamada-Ogatta, A. G. de Oliveira and G. Andrade, *Curr. Pharm. Biotechnol.*, 2016, **17**, 389–397; L. Taghizadeh, M. Montazerozohori, A. Masoudiasl, S. Joohari and J. M. White, *Mater. Sci. Eng. Carbon*, 2017, **77**, 229–244.
4 A. Tamilselvi and G. Mugesh, *J. Biol. Inorg. Chem.*, 2008, **13**, 1039–1053; C. Ribeiro, S. C. Lopes and P. Gameiro, *J. Membr. Biol.*, 2011, **241**, 117–125; A. Tarushi, E. Polatoglu, J. Kljun, I. Turel, G. Psomas and D. P. Kessissoglou, *Dalton Trans.*, 2011, **40**, 9461.
5 K. J. Humpreys, A. J. Jonhson, K. D. Karlin and S. E. Rokita, *J. Biol. Inorg. Chem.*, 2002, **7**, 835; M. Gonzalez-Alvarez, G. Alzuet, J. Borras, M. Pitié and B. Meunier, *J. Biol. Inorg. Chem.*, 2003, **8**, 644; L. Li, K. D. Karlin and S. E. Rokita, *J. Am. Chem. Soc.*, 2005, **127**, 520.
6 J. B. Tommasino, F. N. R. Renaud, D. Luneau and G. Pilet, *Polyhedron*, 2011, **30**, 1663–1670; J. B. Tommasino, G. Pilet, F. N. R. Renaud, G. Novitchi, V. Robert and D. Luneau, *Polyhedron*, 2012, **37**, 27–34.
7 E. Erin and M. D. Connors, *Primary care update*, 1998, **5**, 32–35; G. Larouche, *Pharmactuel*, 2001, **34**, 40–46; A. M. Emmerson and A. M. Jones, *J. Antimicrobial Chem.*, 2003, **50**, 13–20; H. Goossens, M. Ferech, R. V. Stichele and M. Elseviers, *Lancet*, 2005, **365**, 579–587; M. K. Bhattacharjee, *Chemistry of antibiotics and related drugs*, Springer, Nature, Switzerland, 2016, pp. 1–24.
8 I. Beloso, J. Borras, J. Castro, J. A. Garcia-Vazquez, P. Perez-Lourido, J. Romero and A. Sousa, *Eur. J. Inorg. Chem.*, 2004, 635–645; M. T. Robak, M. A. Herbage and J. A. Ellman, *Chem. Rev.*, 2010, **110**, 3600–3740; F. A. Saad and M. A. Khedr, *J. Mol. Liq.*, 2017, **231**, 572–579.
9 G. Psomas and D. P. Kessissoglou, *Dalton Trans.*, 2013, **42**, 6252.
10 F. Bricaire, *Rean. Urg*, 1997, **6**, 3s–8s.
11 Y. Xie, Y. He, P. L. Irwin, T. Jin and X. Shi, *Appl. Environ. Microbiol.*, 2011, **77**, 2325–2331; J. Paquet, Y. Chevalier, J. Pelletier, E. Couval, D. Bouvier and M.-A. Bolzinger, *Colloids Surf., A*, 2014, **457**, 263–274.
12 E. M. Nolan and S. J. Lippard, *Acc. Chem. Res.*, 2009, **42**, 193–203.

13 B. L. Vallee, *Adv. Protein Chem.*, 1955, **10**, 317–384; K. A. Mc Call, C. C. Huang and C. A. Fierke, *J. Nutr.*, 2000, **130**, 1437S–1446S; K. L. Haas and K. J. Franz, *Chem. Rev.*, 2009, **109**, 4921–4960; M. L. Zastrow and V. L. Pecoraro, *Biochemistry*, 2014, **53**, 957–978; Y. Yoshikawa and H. Yasui, *Curr. Top. Med. Chem.*, 2012, **12**, 210–218; N. J. Pace and E. Weerapana, *ACS Chem. Biol.*, 2014, **9**, 258–265.

14 J. J. Recillas Mota, M. J. Bernad, J. A. Mayoral-Murillo and J. Gracia Mora, *React. Funct. Polym.*, 2013, **73**, 1078–1085.

15 A. Tarushi, C. P. Raptopoulou, V. Psycharis, A. Terzis, D. P. Kessissoglou and G. Psomas, *Bioorg. Med. Chem.*, 2010, **18**, 2678–2685.

16 A. Tarushi, K. Lafazanis, J. Kljun, I. Turel, A. A. Pantazaki, G. Psomas and D. P. Kessissoglou, *J. Inorg. Biochem.*, 2013, **212**, 53–65.

17 J. L. Zhang, J. Yang, X. Wang, H. Y. Zhang, X. L. Chi, Y. Chen, Q. Yang and D. R. Xiao, *Z. Anorg. Allg. Chem.*, 2015, **641**, 820–825.

18 J. Barbosa, R. Bergès and V. Sanz-Nebot, *J. Chromatogr.*, 1998, **823**, 411–422; D. Barron, E. Jimenez-Lanzano, A. Irles and J. Barbosa, *J. Chromatogr.*, 2000, **871**, 381–389; V. Sanz-Nebot, I. Toro and J. Barbosa, *J. Chromatogr.*, 2001, **933**, 45–56; J. Barbosa, D. Barron, J. Cano, E. Jimenez-Lazano, V. Sanz-Nebot and I. Toro, *J. Pharm. Biomed. Anal.*, 2001, **24**, 1087–1098; C.-E. Lin, Y.-J. Deng, W.-S. Liao, S.-W. Sun, W.-Y. Lin and C.-C. Chen, *J. Chromatogr.*, 2004, **1051**, 283–290.

19 J. B. Tommasino, G. Chastanet, B. Le Guennic, V. Robert and G. Pilet, *New J. Chem.*, 2012, **36**, 2228–2235.

20 M. P. Lopez-Gresa, R. Ortiz, L. Perello, J. Latorre, M. Liu-Gonzalez, S. Garcia-Granda, M. Perez-Priede and E. Canton, *J. Inorg. Biochem.*, 2002, **92**, 65–74; M. Zampakou, M. Akrivou, E. G. Adreadou, C. P. Raptopoulou, V. Psycharis, A. A. Pantazaki and G. Psomas, *J. Inorg. Biochem.*, 2013, **121**, 88–99.

21 M. T. Alghamdi, A. A. Alssibai, M. S. Shahawi and M. S. Refat, *J. Mol. Liq.*, 2016, **224**, 571–579.

22 G. B. Deacon and R. J. Phillips, *Coord. Chem. Rev.*, 1980, **33**, 227–250.

23 (*a*) E. K. Efthimiadou, A. Karaliota and G. Psomas, *Polyhedron*, 2008, **27**, 1729–1738; (*b*) K. C. Skyrianou, V. Psycharis, C. P. Raptopoulou, D. P. Kessissoglou and G. Psomas, *J. Inorg. Biochem.*, 2011, **105**, 63–74; (*c*) M. E. K. Efthimiadou, Y. Sanakis, M. Katsarou, C. P. Raptopoulou, A. Karaliota, N. Katsaros and G. Psomas, *J. Inorg. Biochem.*, 2006, **100**, 1378–1388; (*d*) H. Ftouni, S. Sayen, S. Boudesocque, I. Dechamps-Olivier and E. Guillon, *Inorg. Chim. Acta*, 2012, **382**, 1378–1388.

24 CrysAlisPro, v. 1.171.33.46 (rel. 27-08-2009 CrysAlis171.NET), Oxford Diffraction Ltd., 2009.

25 (*a*) H. Tompa Demeulenaer, *Acta Crystallogr.*, 1965, **19**, 1014–1018; (*b*) R. H. Blessing, *Acta Crystallogr., Sect. A: Found. Crystallogr.*, 1995, **51**, 33–38.

26 A. Altomare, M. C. Burla, M. Camalli, G. L. Cascarano, C. Giacovazzo, A. Guagliardi, A. G. G. Moliterni, G. Polidori and R. Spagna, *J. Appl. Crystallogr.*, 1999, **32**, 115–119.

27 D. J. Watkin, C. K. Prout, J. R. Carruthers and P. W. Betteridge, in *CRISTAL Issue 11, Vol. CRISTAL Issue 11*, Chemical Crystallography Laboratory, Oxford, UK, 1999.

 